

Mechanical and Thermal Behaviour of Polypropylene/Cloisite 30B/Elvaloy AC 3427 Nanocomposites Processed by Melt Intercalation Method

D. Jafrey Daniel¹ · K. Panneerselvam¹

Received: 23 February 2016 / Accepted: 13 May 2016 / Published online: 27 May 2016
© The Indian Institute of Metals - IIM 2016

Abstract The applications of polymers have increased in last decade by blending it with certain type of fillers, which is a common way to develop polymer nano composites. In this study, polypropylene (PP) as a thermoplastic matrix, Cloisite30B (C30B) (1, 2, 3, 5 wt%) as nano filler and Elvaloy AC 3427 (EA) (15 wt%) as a compatibilizer were processed using a Twin screw extruder. The specimen preparation for testing samples according to ASTM standards were carried out by Injection molding process. The processed PP/C30B/EA nanocomposites were characterized using X-ray diffraction, tensile, flexural, impact, differential scanning calorimetry and Thermogravimetric analysis. X-ray diffraction revealed that the addition of EA to PP/C30B increased d-spacing which formed an intercalated structure. The low addition of C30B to PP matrix enriched the tensile, flexural and impact properties due to their fine dispersion. The high addition of C30B to PP matrix boosted digital scanning calorimetry and thermogravimetric analysis due to the agglomerated structure which was also confirmed by field emission scanning electron microscope studies.

Keywords Adhesion · Compatibilizer · Thermal Properties · Extrusion

1 Introduction

Polymer nanocomposites (PNC) have been investigated by many people from various sectors in recent years due to their increased mechanical, thermal, barrier, flame retardant and excellent corrosion resistance. The properties of virgin polymers can be improved by incorporating fillers into them. PNC's exhibit many dominant properties when compared to the virgin polymers [1, 2]. The quantity of the addition of fillers varies according to the filler used in the matrix. Usually, the nanoclays are added up to 2–5 % by weight while the conventional fillers are added up to 30–40 % by weight [3, 4].

The preparation of PNC is done by melt Intercalation, solvent mixing, solid state mixing and Template synthesis as shown in Fig. 1. Although there are several methods for preparing PNC's, melt intercalation method is often used for its preparation [5]. Melt intercalation is either carried out using Brabender Plasticorder [6] or Extruders [1]. Single or twin screw Extruders are commonly used for nanocomposite preparation. The good mixing characteristics and efficiency of the process makes the extruder more advantageous than other production methods. During the melt intercalation process, the mixture of polymer and the nanoclays are beyond the softening point of the polymer which achieves a uniform dispersion of filler in matrix [1, 2].

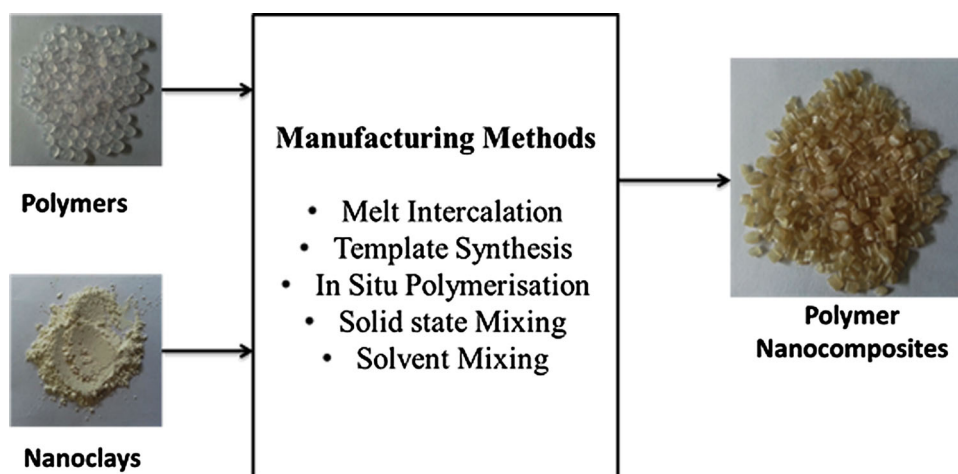
Polypropylene (PP) is an essential commodity thermoplastic which is used in many industries like ropes, automobile and aerospace industries. Polypropylene is a thermoplastic polymer of polypropylene monomer. It is mostly used because of their low cost, better thermal stability and easy processing capabilities [1, 7].

PP is usually reinforced with nanoclays as it has an advantage in forming a nanocomposite structure [8–12].

✉ K. Panneerselvam
kps@nitt.edu

¹ Department of Production Engineering, National Institute of Technology, Tiruchirappalli, Tamil Nadu 620015, India

Fig. 1 Manufacturing Methods of PNC's



The nanoclays have a plate morphology and high aspect ratio. The main challenge while using PP and nanoclays is to achieve effective dispersion of nanoclays in the PP matrix. PP is hydrophobic in nature, whereas clay is naturally hydrophilic in nature which makes the dispersion of clays in PP matrix a difficult task. To overcome these dispersion problems, several researchers have used several types of compatibilizer. Compatibilizer is used to increase the interfacial contact with PP and the nanoclays [13–16]. The main aim of the compatibilizer is to increase the polarity of the PP matrix and to increase the d-spacing of the nanoclays.

Wang et al. [17] added organo-montmorillonite to the PP matrix and they concluded that there was an increase in melting point of the resulting nanocomposite. Li et al. [18] prepared PP/MMT blends with the added addition of maleic anhydride grafted low isotactic homo polypropylene elastomer and observed better dispersion. Lertwimolnun et al. [19] found that the degree of dispersion got enhanced with the addition of PP-g-MA by 10 % weight. They also found that the dispersion was not effective when PP-g-MA was added beyond 25 % by weight. Several other authors added different compatibilizer and found that there was an increase in properties when the addition was added up to a certain limit [20–23].

In this work PP was used as a matrix and C30B as a nano filler. To increase the dispersion effect, a new type of compatibilizer namely EA was added to PP/C30B. The twin screw extruder was used for preparing the PP/C30B/EA nanocomposites. The testing samples were prepared according to ASTM standards by injection molding process. XRD was conducted to find out the structure formed in PP/C30B/EA nano composites. The mechanical properties like tensile, flexural and impact test were studied. The dispersion studies were conducted using field emission scanning electron microscope (FE SEM) to study the

dispersion characteristics of C30B in PP matrix in the presence of EA as compatibilizer. Thermal tests like differential scanning calorimetry (DSC) and thermogravimetric analyser (TGA) were also studied in this paper. The amount of filler content which influenced the various properties was also studied as a main effect in this paper.

2 Experimental

2.1 Materials

PP was used as a thermoplastic polymer which was procured from Reliance with the grade name Repol H110MA with a Melt flow index of 11 g/10 min. The C30B was used as a nano filler which was supplied by Southern Clays and their FE SEM image is shown in Fig. 2. The EA was used as a compatibilizer which was supplied by Du Pont. It was a combination of ethylene and butyl acrylate with a Melt

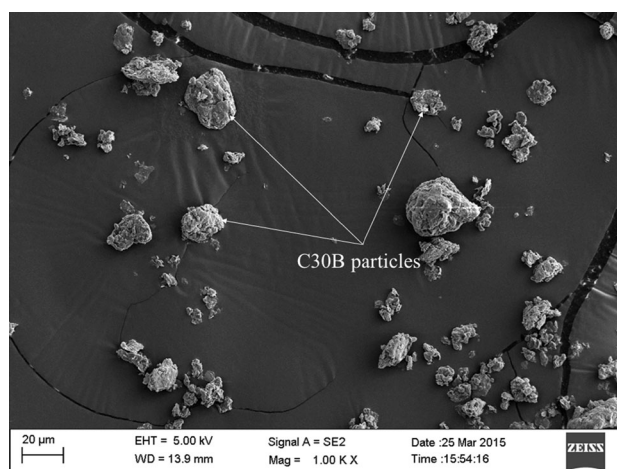


Fig. 2 FE SEM image of C30B

flow index of 4 g/10 min and the density of 0.926 g/cm³. The EA was used to upsurge the dispersion of C30B in PP matrix. The percentage of C30B was varied at 1, 2, 3, 5 wt% in PP matrix. The EA percentage was kept constant at 15 wt% in all additions of C30B in the production of PP/C30B/EA nanocomposites.

2.2 Sample Preparation

2.2.1 Compounding

The Twin screw extruder with an L/D ratio of 40 was used for the processing of PP/C30B/EA nanocomposites. The screw RPM was set to 65 and the temperature of the blocks was kept from 170 to 220 °C (i.e. from feed area to die area). The twin screw extruder had different zones like conveying zone, melting zone, mixing zone and plasticizing zone. As the material passed through these zones of the twin screw extruder, there was a decrease in screw pitch which helped the C30B to get reinforced with PP matrix. The strands of 3 mm diameter from the die area were air and water cooled and it was cut into 3 mm length by a pelletizer.

2.2.2 Specimen Preparation

The samples for testing were injection molded using a horizontal type injection molding in which the barrel temperature was set at 170 to 190 °C. The injection time was set to 5 s and it was water cooled for 80 s. The injection pressure was maintained at 90 bars and die locking pressure was maintained at 130 bars [1].

3 Characterization of Processed PP/C30B/EA Nanocomposites

3.1 XRD

XRD was conducted to find out the structure formation in PP/C30B/EA nanocomposites. XRD machine was equipped with Rigaku generator using Cu K_α radiation with the wavelength of 0.154 nm and the scanning angle was between 5° and 80°. The d spacing of the interlayer gallery of C30B and PP/C30B/EA nanocomposites was calculated using the Bragg's equation ($n\lambda = 2d\sin\theta$).

3.2 Morphological Studies

The dispersion of C30B in the PP matrix was studied using FE SEM. The samples for FE SEM was gold sputtered to make the sample conductive.

3.3 Tensile, Flexural and Impact Tests

The tensile strength of the PP/C30B/EA nanocomposites was carried out according to ASTM D638-14 standards. The cross head speed was maintained at 5 mm/min. The toughness of the PP/C30B/EA nanocomposites was evaluated using Notched Charpy test according to ASTM D256-10 standard with a hammer force of 6.5 J. The bending properties of the PP/C30B/EA nanocomposites were evaluated using three point bending test in accordance with ASTM D790-10 standards with a crosshead speed of 2 mm/min.

3.4 Thermogravimetric Analysis (TGA)

The thermal stability of PP/C30B/EA nanocomposites was checked using the thermogravimetric analysis using TGA 4000 Perkin Elmer. TGA was used for checking weight loss with respect to rise in temperature for raw material and finished product. The sample weight was approximately 5 mg. The gas flow rate was 20 ml/min; gas used was nitrogen; temperature rise was 10 °C/min and maximum test temperature –600 °C for which 180 µl platinum pan was used.

3.5 Digital Scanning Calorimetry (DSC)

Differential scanning calorimeter was measured using DSC 6000—PerkinElmer apparatus. This unit had a single furnace and followed the principle of heat flux. The furnace material was made of alumina coated aluminium, pyris software was used to record the results, the calorimetric performance followed the dynamic range of ±175 mW with accuracy ±2 % and precision ±0.1 %. The operating temperature was from room temperature to 220 °C. The gas flow rate was 20 ml/min, heating rate was 10 °C/min and was maintained in Nitrogen environment.

4 Results and Discussion

4.1 XRD

XRD are the commonly used technique for finding out the structure of the polymer nanocomposites. XRD have been used for finding out the structure of PP/C30B/EA nanocomposites by examining the shape, intensity of basal reflection and the position of the peaks. The XRD results of C30B and PP/C30B/EA nanocomposites are shown in the Fig. 3. The 2θ values of the C30B and the PP/C30B/EA nanocomposites are given in the Table 1.

From Fig. 3 it is observed that, there is a repetitive multiple layer structure which helps to find the d-spacing of the PP/C30B/EA nanocomposites. The initial peak of the

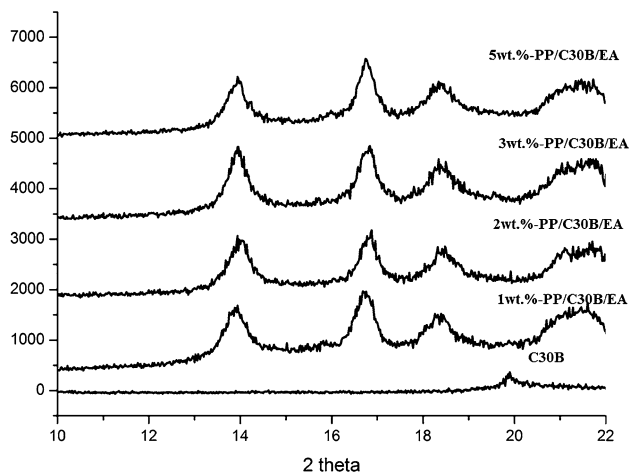


Fig. 3 XRD patterns of C30B and PP/C30B/EA nanocomposites in stated proportions

Table 1 The 2θ values for C30B and various percentages of PP/C30B/EA polymer nanocomposites stated in their proportions

C30B	1 wt%	2 wt%	3 wt%	5 wt%
19.88	6.13	6.14	6.15	6.11
	13.94	13.95	13.95	13.97
	16.71	16.86	16.86	16.75
	18.39	18.39	18.42	18.33
	21.04	21.76	21.76	21.81

C30B is found at 19.98° with the d-spacing of 4.46 \AA . The initial peak values of the PP/C30B/EA nanocomposites are found at 6.13° , 6.14° , 6.15° , 6.11° with the d-spacings 14.40 , 14.45 , 14.45 , 14.46 \AA respectively. The 2θ values of the PP/C30B/EA nanocomposites decreases while there is an increase in d-spacing when compared to the C30B which confirms the formation of polymer nanocomposites. The increase in the d-spacing is mainly due to the addition of EA type compatibilizer to PP and C30B. In comparison with the peak of C30B, the peak of PP/C30B/EA nanocomposites is shifted to the lower angles which confirms the formation of the intercalated structure [1] as shown in Fig. 3.

4.2 Tensile Studies

The Stress–Strain graph is shown in Fig. 4 and, Ultimate tensile strength and Young's Modulus, of the various percentage of PP/C30B/EA nanocomposites is shown in Fig. 5. It can be noted that on increasing the C30B content up to 2 wt% in PP matrix, the ultimate tensile strength increases continuously. The main reason for the improvement of ultimate tensile strength is mainly due to the possible delamination of C30B galleries. The ultimate

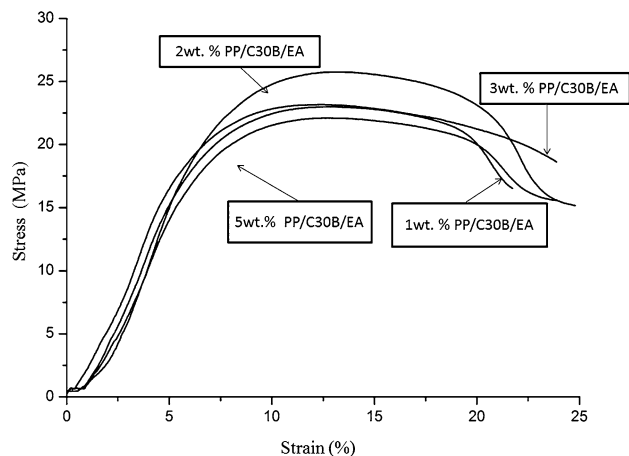


Fig. 4 Stress strain curve of PP/C30B/EA nanocomposites in stated proportions

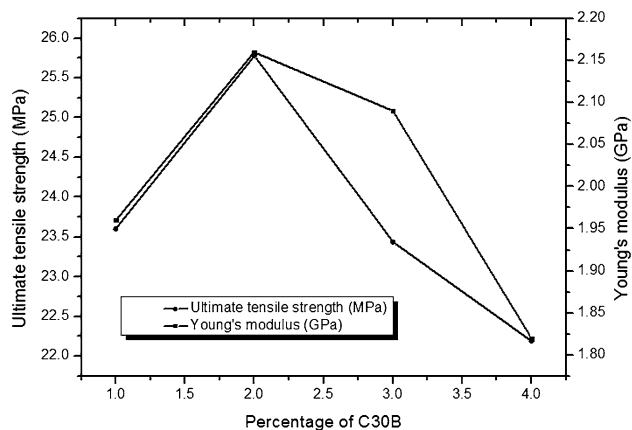


Fig. 5 Percentage of C30B versus ultimate tensile strength (MPa) and Young's Modulus (GPa)

tensile strength can be easily related to the FE SEM observations. The improvement in ultimate tensile strength can be attributed to the presence of immobilized PP polymer phases which may be due to the result of the interaction of PP polymer phases with C30B and the fine dispersion of C30B in PP matrix as shown in Fig. 6. The other plausible reason can be the orientation of the C30B along the tensile direction which may have also resulted in higher ultimate tensile strength at 2 wt%. The Ultimate tensile strength and the Young's modulus of PP/C30B/EA nanocomposites increases at 2 wt% which may be due to the better intercalated structure in it.

On increasing the C30B content in PP matrix beyond 2 wt%, a decrease in ultimate tensile strength and young's modulus can be observed. This decreasing pattern may be due to the C30B–C30B interaction which results in agglomerated structure as shown in Fig. 7. These agglomerated structure gives rise to local stress concentration in PP/C30B/EA nanocomposites which results in

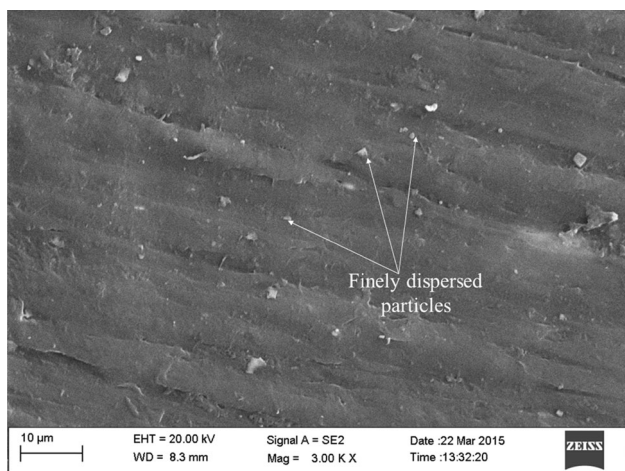


Fig. 6 FE SEM image of 2 wt% PP/C30B/EA

reduction of aspect ratio of clay, resulting in reduced contact surface between the C30B and the PP matrix. Thus the C30B addition from 3 to 5 wt% results in reduced ultimate tensile strength and young’s modulus when subjected to tensile testing. The likely reason for the formation of the agglomerated structure is due to the presence of the large concentration of PP which does not mingle with the C30B. As the result of agglomeraration the C30B are stacked together and there is no delamination of layers in it.

4.3 Flexural Test

The flexural strength of PP/C30B/EA nanocomposites are shown in Fig. 8. During the flexural test, the upper half of the specimen is in compression and the lower half of the specimen is in tension which makes the crack propagation difficult on the tension side. This makes the values of flexural strength more than tensile strength.

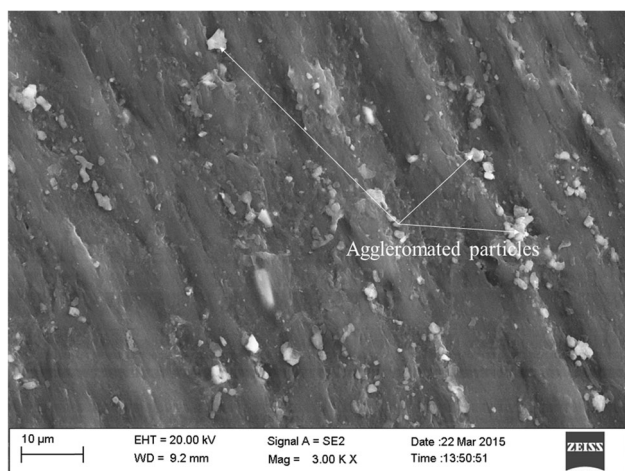


Fig. 7 FE SEM image of 5 wt% PP/C30B/EA

The C30B addition is responsible for the increase in stiffness while the PP matrix and EA addition are responsible for the increase in flexural strength. A behaviour related to the tensile strength studies has also been observed in flexural strength studies. In this study the highest value of flexural strength is found at 2 wt% of C30B addition, which may be due to the intercalated structure formed in PP/C30B/EA nanocomposites.

The addition of C30B to the PP matrix forms a stiffening effect which may also be a reason for the upsurge in flexural strength and flexural strain at 2 wt%. From Fig. 6, it can be inferred that the homogeneous dispersion of the C30B in PP matrix and the good adhesion of C30B in the PP matrix also increases the flexural strength at 2 wt%. The other plausible reason for the decrease in flexural strength may be due to the particle agglomeration of C30B in PP matrix as shown in Fig. 7.

4.4 Impact Properties

The impact strength of various PP/C30B/EA nanocomposites is shown in Fig. 9. The impact strength varies according to the structure of the PP matrix and the amount of reinforcement of C30B. The impact strength initially increases up to 3 wt% addition of C30B but with further addition it decreases. The immiscible aggregates of the clay act as a stress concentrator, which leads to failure even if they are at low level of addition of C30B to PP matrix. The other probable reason for the decrease in impact strength may be due to the reduced toughness of EA relative to PP due to their low molar mass. When the C30B content is more than 3 wt%, the density of the resulting PP/C30B/EA nanocomposites are higher and it leads to the

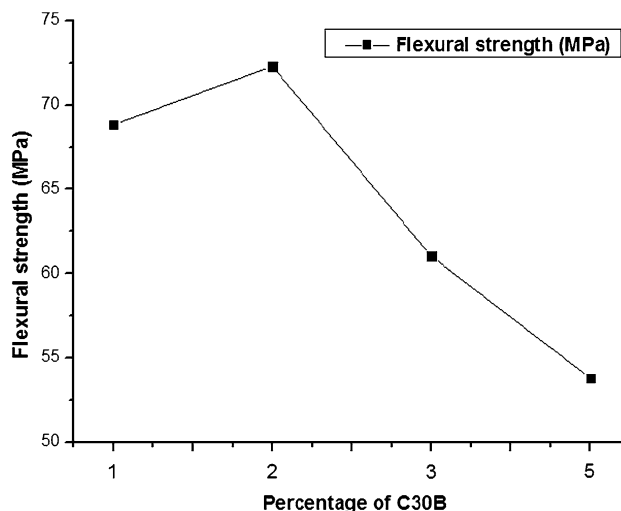


Fig. 8 Percentage of C30B versus flexural strength (MPa) of PP/C30B/EA nanocomposites in stated proportions

increase in the inter particle distance which decreases the impact strength (Fig. 10).

4.5 Differential Scanning Calorimetry (DSC)

The glass transition temperature (T_g) of the processed PP/C30B/EA nanocomposites has been studied using DSC. Figure 11 shows the DSC heating thermograms of various percentages of PP/C30B/EA nanocomposites. When the addition of C30B increases there is a marginal increase in T_g as shown in Table 2 which confirms that the C30B can act as a nucleating agent [24]. According to Chao et al. [25], the addition of compatibilizer has a minimum effect of T_g . Thus the addition of 5 wt% of C30B to the PP matrix shows an increase in T_g value which may be due to the agglomerated structure formed in the resulting nanocomposites as shown in Fig. 7.

4.6 Thermogravimetric Analysis (TGA)

TGA method is commonly applied to polymers/polymer nanocomposites which are used for finding their thermal properties. Due to the distinctive structure of layers in a polymer matrix, their shape and reinforcement dimensions close to the nano level, numerous effects have been observed that can define the changes in thermal properties. Several authors have also found that the addition of fillers to the virgin polymers have enhanced the thermal stability of the polymers [26–28]. It is well known that PNC's increases the thermal stability which is mainly due to the formation of char which delays the diffusion of the volatile decomposition products, as a direct result of the shrinkage in permeability. The exact degradation cannot be predicted because it depends upon the addition of fillers to the polymer [24]. The TGA thermograms of various

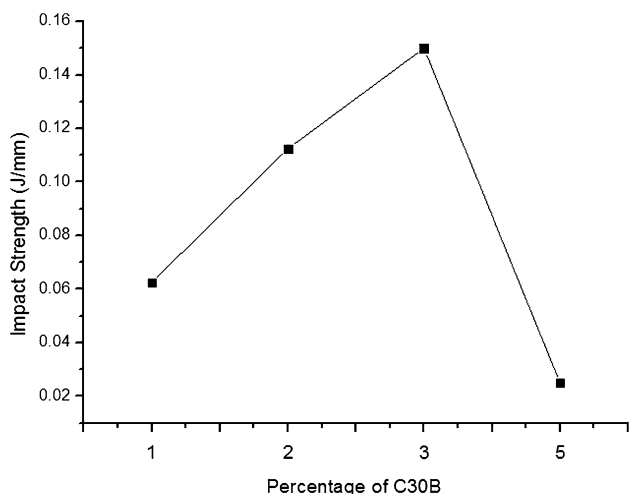


Fig. 9 Percentage of C30B versus impact strength (J/mm) of PP/C30B/EA nanocomposites in stated proportions

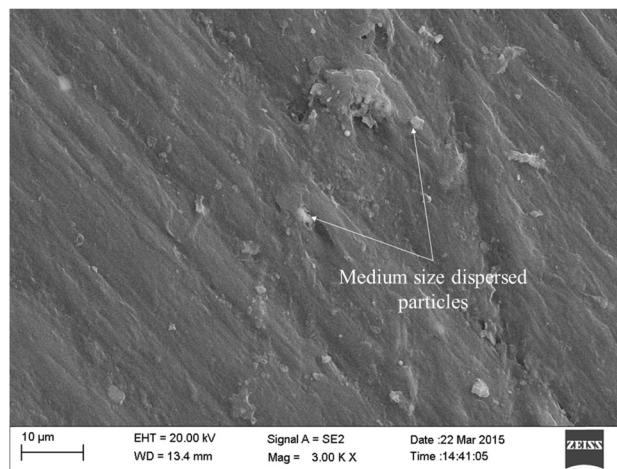


Fig. 10 FE SEM image of 3 wt% PP/C30B/EA polymer nanocomposites

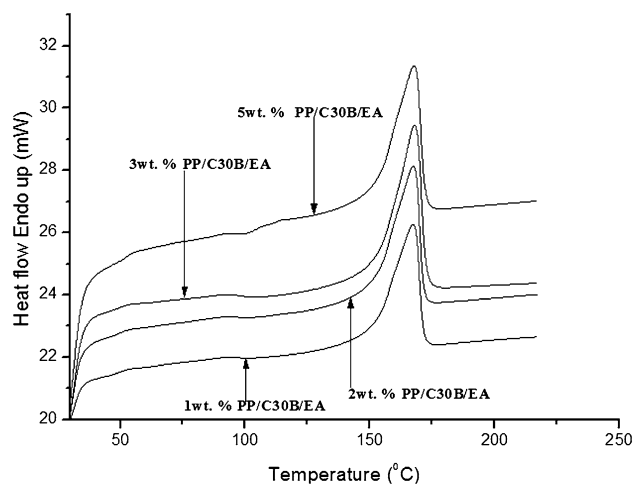


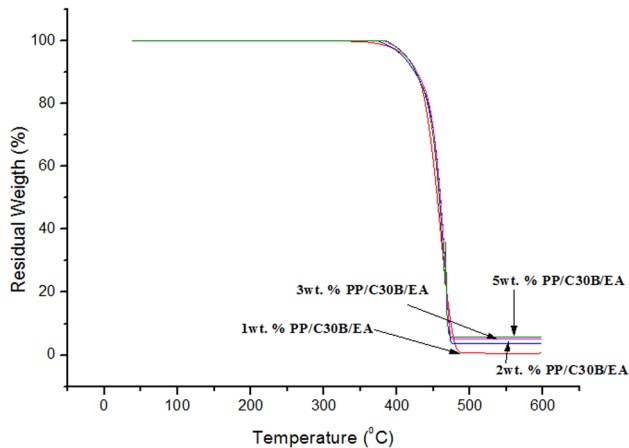
Fig. 11 DSC thermograms of PP/C30B/EA nanocomposites in stated proportions

percentages of PP/C30B/EA nanocomposites is shown in Fig. 12. The Onset temperature, Decomposition temperature and Char residue at 600 °C are given in the Table 3.

The chemical nature of the polymers and the effective stress transfer between the C30B and the PP matrix plays a vital role in determining the thermal stability of the polymers. In this study, the addition of C30B to the PP matrix forms an intercalated structure in it as shown in Fig. 3. With the addition of low amount of C30B to PP matrix (i.e. 1 wt%), there is a domination of intercalation particles, but it is not sufficient to enhance the thermal stability of the resulting PP/C30B/EA nanocomposites. At the highest level of addition of C30B to PP matrix (i.e. 5 wt%), there are more intercalated clay particles which can increase the char formation in the resulting PP/C30B/EA nanocomposites as shown in Table 3.

Table 2 Glass transition temperature (T_g) of the PP/C30B/EA nanocomposites in stated proportions

Materials	Glass transition temperature (T_g) (°C)
1 wt% PP/C30B/EA	167.37
2 wt% PP/C30B/EA	167.49
3 wt% PP/C30B/EA	167.59
5 wt% PP/C30B/EA	167.83

**Fig. 12** TGA thermograms of PP/C30B/EA nanocomposites in stated proportions**Table 3** Onset temperature (°C) and decomposition temperature (°C) of PP/C30B/EA nanocomposites in stated proportions

Materials	Onset temperature (°C)	Decomposition temperature (°C)	Char residue at 600 °C (%)
1 wt% PP/C30B/EA	349.75	459.75	99.378
2 wt% PP/C30B/EA	350.62	464.62	96.278
3 wt% PP/C30B/EA	354.67	465.74	94.935
5 wt% PP/C30B/EA	357.78	466.78	94.224

5 Conclusion

1. In this study PP/C30B/EA nanocomposites were successfully prepared by Twin Screw Extruder. The XRD studies revealed that there was an intercalated structure formed as there was an increase in d-spacing values and decrease in 2θ values.
2. The FE SEM studies revealed that there was a uniform dispersion of fillers in polypropylene matrix at 2 wt% addition of C30B and an agglomerated structure formed at an addition of 5 wt% of C30B to PP matrix in the presence of EA as compatibilizer.

3. The optimum tensile strength and flexural strength was found with an addition of 2 wt% C30B to the PP matrix which was mainly due to the fine dispersion of C30B in PP matrix and strong interaction between them.
4. The impact strength increased up to 3 wt% addition of C30B to PP matrix beyond which it decreased. The reason for reduction in its value was mainly due to the transformation from ductile to brittle form at higher loading.
5. The DSC and TGA test revealed that there was an increase in thermal properties with the addition of 5 wt% of C30B to the PP matrix. The presence of agglomerated structure increased the thermal properties.
6. Thus the lower level of additions of C30B to PP matrix was suitable for mechanical applications while the higher level of addition of C30B to PP matrix was suitable for thermal based applications. Thus the amount of reinforcement was selected based on the end use applications.

References

1. Daniel D J and Panneerselvam K, (2015). *J Compos Mater*, 0021998315616176.
2. Ray S and Okamoto, *Progr Polym Sci* **27** (2003) 1539.
3. Zhou Y, Rangari V, Mahfuz H, Jeelani S and Mallick P K, *Mat Sci Eng A-Struct* **402**(2005) 109.
4. Ellis T S and D'Angelo J S J, *Appl Polym Sci* **90** (2003) 1639.
5. Maniar K K, *Polym Plast Technol* **43** (2004) 427.
6. Touati N, Kaci M, Bruzaud, S, and Grohens Y, *Polym Degrad Stabil* **96** (2011) 1064.
7. Lee S T CRC Press, Boca Raton, FL (2000) p 71.
8. Doroudiani S, Park C B and Kortschot M T, *Polym Eng Sci* **38** (1988) 1205.
9. Rachtanapun P, Selke S E and Matuana L M, *Polym Eng Sci*, **44** (2004) 1551.
10. Liu W, Liu B, and Wang, X, *Int J Polym Mater* **62** (2013) 164.
11. Lai S-M, Chen W-C and Zhu X S, *Compos Part A-Appl S* **40** (2009) 754.
12. McCallum T J, Kontopoulou M, Park C B, Muliawan E B and Hatzikiriakos S G, *Polym Eng Sci* **47** (2007) 1133.
13. Creton C, Kramer E J, Hui CY and Brown H R, *Macromolecules* **25** (1992), 3075.
14. Kim S J, Shin B S, Hong J L, Cho W J, Ha C S, *Polymer* **42** (2001) 4073.
15. Boucher E, Folkers J P, Hervet H, Leger L and Creton C, *Macromolecules* **29** (1996) 774.
16. Wang T, Liu D and Xiong C J, *Mater Sci* **42** (2007) 3398.
17. Wang Y, Zhang Q, Fu Q, *Macromol Rapid Commun* **24** (2003) 231.
18. Li J, Zhou C X Wang G, Yu W, Tao Y and Liu Q, *Polym Compos* **24** (2003) 323.
19. Lertwimolnun W and Vergnes B, *Polymer* **46** (2005) 3462.
20. Lim S H, Dasari A, Wang G T, Yu Z Z, Mai Y W, Yuan Q, and Yong M S, *Compos Part B-Eng* **41** (2010) 67.

21. Chinellato A C, Vidotti S E, Hu G H, and Pessan L A, *Compos Sci Technol* **70** (2010) 458.
22. Zhang S, Hull T R, Horrocks A R., Smart G, Kandola B K, Ebdon J and Hunt B, *Polym Degrad Stabil* **92** (2007) 727.
23. Shokoohi S, Arefazar A, and Naderi G, *Mater Design* **32** (2011) 1697.
24. Iyer R, Suin S, Shrivastava N K, Maiti S, and Khatua B B, *Polym-Plast Technol* **52** (2013) 514.
25. Ding C, Jia D, He H, Guo B and Hong H, *Polym Test* **2005** **24** (2005) 94.
26. Chow W S, Tham W L, *Polym-Plast Technol* **48** (2009) 342.
27. Modesti M, Lorenzetti A, Bon D and Besco S, *Polym Degrad Stabil* **91** (2005) 672.
28. Qin H L, Zhang S M, Zhao C G, Feng M, Yang M S, Shu ZJ and Yang S S, *Polym Degrad Stabil* **85** (2004) 807.